

Numerical Simulation of Facility Effects on Hall Thruster Performance

John Michael Fife

Manuel Martinez-Sanchez*
Massachusetts Institute of Technology
Cambridge, Massachusetts

In order to study physical processes in Hall thrusters, an evolved hybrid particle-in-cell (PIC) numerical model, HPHall, was developed. A set of quasi-one-dimensional fluid equations is used for electrons, and a particle-tracking Boltzmann solver is used for the heavy species. The two systems are linked by charge neutrality. Background density is modeled as a uniform flux of neutral particles across the downstream boundary into the domain equivalent to the thermal flux. The results are used to examine the effect of facility background pressure on efficiency. A simple formula for the change in measured utilization efficiency versus facility pressure is also presented. This model agrees well with the numerical results. Although the trend is correct, the experimental data shows efficiency increasing much more rapidly with facility pressure. The discrepancy is believed to be due to physical mechanisms that are not included in the simple model, such as those driving anomalous diffusion.

Introduction

To predict the on-orbit performance of Hall thrusters, measurements are routinely made in vacuum chambers. However, due the difficulty in pumping chambers to very low vacuums during thruster operation, these measurements are often made at atom number densities around $6 \cdot 10^{17} m^{-3}$, which is much higher than that of the space environment ($\sim 10^{14} m^{-3}$ at LEO). Furthermore, these chamber densities are on the order of the atom density in parts of the acceleration channel. Therefore, it is natural to believe that p_b may have an effect on thruster performance.

Experimental studies have investigated this. Performance measurements for the same thruster have been found to vary significantly with chamber pressures between 10^{-5} and 10^{-4} Torr.^{1,2}

Numerical simulations of Hall thrusters have also been developed.^{3,4} This paper describes the use of one such simulation, *HPHall*, used here to examine the effects of facility pressure on thruster performance. *HPHall* is a two-dimensional transient hybrid particle-in-cell (hybrid PIC) simulation for Hall thrusters. Descriptions of *HPHall* have been presented before⁵⁻⁸, and a summary of the model and method will be repeated here for completeness.

Governing Equations

Although this transient 2-D 3-V simulation operates in cylindrical coordinates $(z, r, v_z, v_r, v_\theta)$, some vector quantities in the analysis below are written with

respect to the magnetic field lines. As Fig. 1 shows, \hat{n} and \hat{t} are used to represent the distance vectors normal and tangent to the magnetic field lines, respectively.

Electrons

The simplified electron equations consist of a generalized Ohm's law, a current conservation equation, and an electron temperature equation. Assuming a Maxwellian electron distribution, quasineutrality, and a particular ion field, these three equations are sufficient to yield electron current density, space potential, and electron temperature as a function of time.

The diffusion coefficient of electrons along magnetic field lines is assumed to be much greater than the diffusion coefficient across them. Ignoring the magnetic mirror effect, and assuming constant electron temperature along magnetic field lines, the momentum equation gives,

$$\phi + \frac{kT_e}{e} \ln(n_e) = \phi^*(\lambda). \quad (1)$$

Note that Eq. (1) holds along magnetic field lines. λ is a magnetic stream function which is constant for any given field line.

Electron diffusion across the magnetic field is assumed to obey a Generalized Ohm's Law. In the lab frame, the cross-field electron velocity in terms of an effective electron mobility across the magnetic field lines, $\mu_{e,\perp}$, is

$$u_{e,\hat{n}} = -\mu_{e,\perp} \left(E_n + \frac{1}{en_e} \frac{\partial p_e}{\partial \hat{n}} \right). \quad (2)$$

*Professor, AIAA Fellow

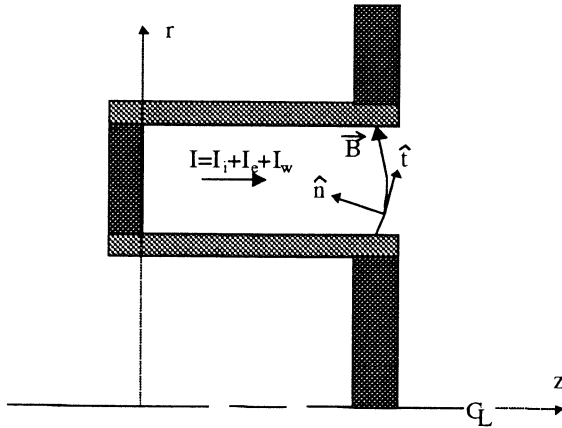


Fig. 1. Diagram showing a simplified Hall thruster discharge channel cross section, the coordinate system used, and the current convention.

Classical cross-field mobility in the weakly ionized limit⁹ ($\sim 1/B^2$) has been shown¹⁰ not to adequately describe the high electron transport across lines of force in the presence of a strong magnetic field. Some previous work has suggested that the discrepancy between measured and predicted mobility may be due to anomalous “Bohm” diffusion,¹¹ which goes as $1/B$. Neither classical nor Bohm models appropriately describe the mobility throughout the discharge channel. It is believed that, in some regions, other mechanisms, such as wall conductivity or wave transport, may dominate. However, in the interest of exploring the physics of the acceleration process, we use classical and Bohm mobility here,

$$\mu_{e,\perp} = \frac{\mu_e}{\beta_e^2} + K_B \frac{1}{16B}, \quad (3)$$

and leave the coefficient, K_B , as an adjustable parameter between 0 and 1. Based on comparison with experimental data, the “best” K_B was found to be .15.

Current Conservation

Since quasineutrality is imposed, no space charge can accumulate, and current must be conserved for the whole device. A conservation equation for current crossing any magnetic field line can be written $I_a = I_e + I_i + I_w$, where I_a , I_e , I_i , and I_w are the discharge, electron, ion, and near-wall currents, respectively. In terms of integrals along magnetic field lines,

$$I_a = -2\pi e \int_0^l n_e u_{e,n} r ds + 2\pi e \int_0^l n_i u_{i,n} r ds + I_w. \quad (4)$$

By combining Eqs. (1) through (4) a differential equation may be obtained for the cross-field variation of ϕ^* .

Electron Energy Equation

An electron energy equation is derived under the assumptions that electrons have a Maxwellian velocity distribution, and that the pressure dyad reduces to a scalar pressure term, $n_e k T_e$. Source terms include losses due to ionization, radiation, and charge-field interactions. Ionization and radiation losses are modeled analytically with a net ion production cost according to Dugan and Sovie.¹² Charge-field interactions are modeled as j_e^2 / σ_e . The energy equation is applied across magnetic field lines only. Along them, electrons are assumed to be isothermal.

Ionization Rate

The bulk electron-neutral ionization rate is determined by integrating the Drawin⁹ cross-section over a Maxwellian electron distribution. This bulk ionization rate, plus the equations of motion for the ions and neutrals, completes the model for those species.

Boundary Conditions

At the insulator wall, all arriving ions are assumed to recombine with electrons from the plasma. The sheath potential, ϕ_w , is calculated by balancing the ion, electron, and secondary electron fluxes as analytic functions and solving for ϕ_w . An analytic equation for electron energy lost to the wall and sheath is obtained by integrating the primary and secondary electron energy fluxes across Maxwellian distributions. This model has been presented before in detail.⁷ The resulting heat flux to the wall is low for T_e less than some breakpoint temperature, $T_{e,bp}$, but develops rapidly above that. In fact, the heat loss grows so large above $T_{e,bp}$ that it becomes an effective limit on electron temperature. For the results presented in this paper, $T_{e,bp} \approx 26 eV$.

Sheath and secondary emission effects are also important when considering cross-field electron transport near the wall. The low-energy secondary electrons are assumed to start from rest at the wall in crossed electric and magnetic fields. By calculating the distance traveled downstream by their guiding centers, an expression for the total near-wall electron conductivity is determined:

$$I_w = e \delta_{eff} \left(\frac{2\pi E m_e}{B^2 \sin(\theta)} \right). \quad (5)$$

Above, δ_{eff} is the effective secondary emission yield, and θ is the angle of incidence of the magnetic field line with the wall.

The electron boundary conditions are handled by directly fixing T_e at the cathode, and by imposing a zero-slope condition on T_e at the anode.

Background (chamber) pressure is modeled at the boundary with a total cross-plane flux of $n_{n,b}\bar{c}/4$, where $n_{n,b}$ is the background number density. The initial velocity distribution of neutrals from the background is set uniformly to the mean thermal speed at 300°K for simplicity.

Numerical Method

The governing equations are solved time-accurately by separating the slow time scale (ion and neutral) motion from the fast time scale (electron) motion, and iterating successively. Individual ion and neutral atoms are simulated using a Particle-In-Cell method. The electron motion is modeled as a fluid continuum with the differential equations derived above and solved using the usual methods.

Runs presented in this paper use a 47-by-22 structured nonuniform grid encompassing the acceleration channel and approximately 4cm of the plume. Rotational symmetry is assumed. Therefore, only a meridional section of the Hall thruster acceleration zone is modeled. Grid spacing is determined by the timestep of the simulation. It is set not to exceed the maximum distance traveled by an ion particle in one timestep.

The magnetic field is generated as a pre-process by specifying the thruster geometry, assuming infinite permeability of the iron poles, and solving Laplace's equation on the regions exterior to the poles. The coils are assumed to be perfect solenoids, so the problem reduces to that of potential flow, with each pole piece set to a given magnetic potential.

The motion of heavy particles is slow compared to the electrons. For computational efficiency, the electrons and heavy particles are moved on different timesteps. Fig. 2 shows the sequence. Since T_e does not vary along magnetic field lines ($T_e = T_e(\lambda)$), it is possible to reduce the electron energy equation to a quasi-one-dimensional form. After some manipulation, a one-dimensional nonlinear differential equation is derived for T_e as a function of λ . The solution of this equation is accomplished by using a modified Forward Time Centered Space (FTCS) method.¹³ The timestep is $5 \cdot 10^{-11}$ seconds, based on successive reduction to the case where the solution is stable and unchanging for smaller timesteps. Once T_e and ϕ^* are known on the domain, ϕ is found using Eqn. (1).

The electric field and electron temperature, determined by integrating the electron equations, is then used in a PIC method for ions and neutrals. Ion positions and velocities are updated. Also, the densities are adjusted appropriately based on

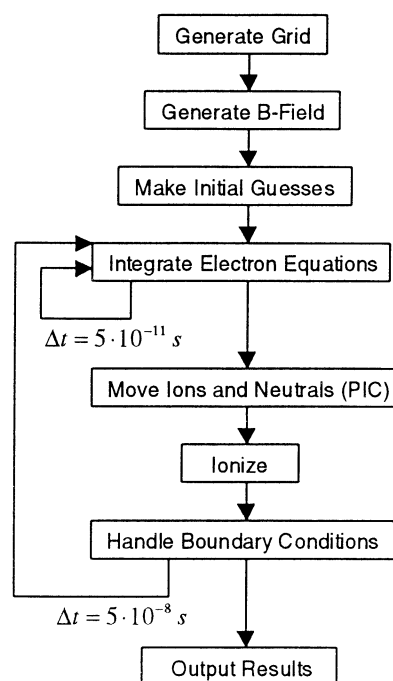


Fig. 2. Execution sequence of the numerical simulation.

computed local bulk ionization rate. This sequence repeats as shown in Fig. 2.

Since the method is time-accurate, the simulation will not, in general, converge to a steady state solution because of plasma fluctuations. Nevertheless, a solution is considered complete when the fluctuations reach a regular frequency and amplitude, and have repeated many periods. For this paper, results are averaged over 0.5ms. One case takes approximately 5 hours to converge on a Pentium II Xeon-class personal computer.

Results and Discussion

Several cases were run to examine the effect of background pressure on Hall thruster operation, as shown in Table 1. Geometry is that of an SPT-70. Operational parameters are $V_d = 300V$ and $\dot{m} = 2.34mg/s$. The first case in Table 1 is experimental, and was run at AFRL.¹⁴ Each numerical case has identical operational parameters, except for the variation in p_b . Efficiencies are for the discharge only, excluding cathode flow. All pressures are for xenon.

A typical plasma density profile from the numerical model is shown in Fig. 3. Ionization peaks near $z = 2.5cm$. The drop-off in density near the exit of the channel is due to acceleration of the ions out the device.

Table 1. Performance results from the numerical simulation, varying background pressure.

| | Experiment | CASE 1 | CASE 2 | CASE 3 | CASE 4 | CASE 5 | CASE 6 |
|--------------|-------------------|--------|---------------------|-------------------|---------------------|-------------------|----------------------|
| p_b (Torr) | $1 \cdot 10^{-5}$ | 0 | $2.5 \cdot 10^{-5}$ | $5 \cdot 10^{-5}$ | $7.5 \cdot 10^{-5}$ | $1 \cdot 10^{-4}$ | $1.25 \cdot 10^{-4}$ |
| I_a (A) | 2.23 | 2.49 | 2.51 | 2.54 | 2.56 | 2.59 | 2.61 |
| I_b (A) | 1.61 | 1.58 | 1.61 | 1.64 | 1.66 | 1.69 | 1.71 |
| F (mN) | 37.8 | 40.7 | 41.3 | 41.9 | 42.4 | 43.1 | 43.6 |
| η_u | 0.936 | 0.921 | 0.936 | 0.953 | 0.966 | 0.983 | 0.996 |
| η_a | 0.720 | 0.636 | 0.640 | 0.644 | 0.647 | 0.651 | 0.654 |
| η_e | 0.677 | 0.809 | 0.806 | 0.802 | 0.799 | 0.796 | 0.793 |
| η | 0.456 | 0.474 | 0.483 | 0.492 | 0.500 | 0.510 | 0.517 |

Breakdown of thrust efficiency may be given by¹⁵
 $\eta = \eta_u \eta_a \eta_e$, where:

$$\begin{aligned}\eta_u &= \frac{I_b m_i}{e \dot{m}} \\ \eta_a &= \frac{I_b}{I_a} \\ \eta_e &= \frac{V_b}{V_d}\end{aligned}\quad (6)$$

Above, I_b is the ion beam current, I_a is the discharge current, V_b is the mean ion beam energy in Volts, and V_d is the discharge Voltage.

Background pressure has the effect of increasing measured efficiency. This is because neutrals from the background are ingested into the thruster channel, where they are used as propellant. A model for the increase in utilization efficiency, η_u , with background pressure may be formulated as,

$$\eta_u' = \frac{\dot{m}_i + \dot{m}_a}{\dot{m}} = \eta_u + \frac{\dot{m}_a}{\dot{m}}, \quad (7)$$

where η_u' represents efficiency measured in a chamber, and \dot{m}_a is the additional propellant (backflow) from the chamber,

$$\dot{m}_a = C_b m_i \frac{n \bar{c}}{4} A. \quad (8)$$

Here, A is the annular area of the acceleration channel (35.9 cm^2 for the SPT-70), and $C_b \approx 1$. For the data of CASE 1 through CASE 6, and for neutral temperatures near ambient (300°K) we find $C_b = 1.13$. This is interesting, since it implies that an additional number greater than $An_{n,b}\bar{c}/4$ are being ionized and ejected in the beam. One possibility is that some are ionized outside the channel – effectively increasing A . This is evidenced by the fact that the beam energy efficiency, η_e , decreases with background pressure. The ions created outside the channel do not contribute much to total beam energy.

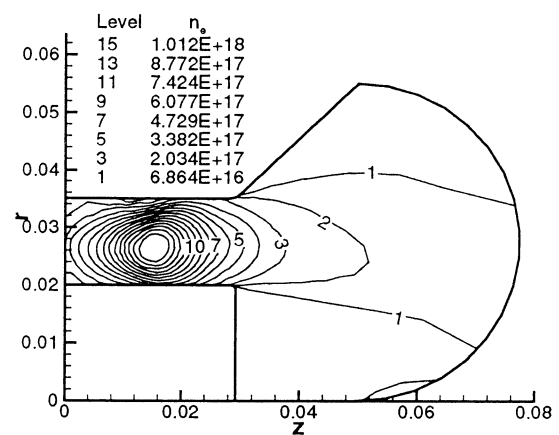


Fig. 3. Plasma density contours for CASE 1.

Another possibility is that the neutral temperature is greater than 300°K , which would increase the backflow rate above what was calculated here. Higher neutral temperatures could be due to high-energy beam ions recombining at the walls without full accommodation to wall temperatures.

Fig. 4 compares the numerical simulation results with experimental data taken at NASA Glenn Research Center with an SPT-100.¹ Although the numerical model is applied to the SPT-70 geometry, comparisons can still be made since the devices are similar.

The operating parameters for the SPT-100 were $V_d = 300 \text{ V}$ and $\dot{m} = 5.13 \text{ mg/s}$. Pressures are the partial pressure of xenon plus the chamber base pressure, which is not reported but is believed to be less than $3 \cdot 10^{-6} \text{ Torr}$ based on a later publication.² Efficiencies are for the discharge only, excluding cathode flow.

The initial rate of increase in measured efficiency is much higher than Eq. (7) predicts using the SPT-100 parameters ($A = 41.4 \text{ cm}^2$). In fact, the rate of

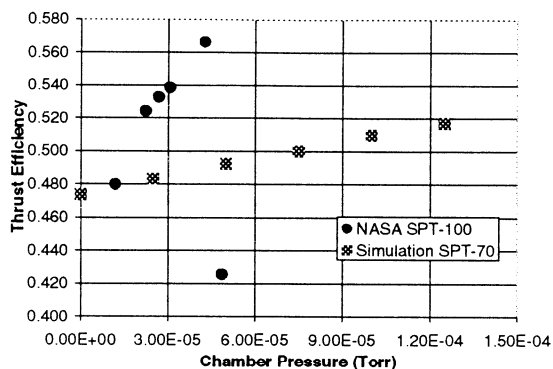


Fig. 4. Thrust efficiency versus chamber pressure from experiment and simulation.

increase would require $C_b \approx 10$. This implies that other processes besides simply backflow utilization are at work. Such processes may change the other efficiency parameters, η_a and η_e , and may be related to those driving anomalous conductivity. Indeed, the SPT-100 discharge characteristics were observed to change significantly with pressure. Discharge current became unstable for chamber pressures greater than $\sim 4 \cdot 10^{-5} \text{ Torr}$, leading to a precipitous drop in performance above that.

Summary

A simple model for change in utilization efficiency with background pressure was formulated in which the backflow of neutral xenon from the chamber is consumed as additional propellant. This model was found to agree well with numerical simulations. However, measured thrust efficiency increased with background pressure more rapidly than expected. This implies that other mechanisms are at work which are not yet identified.

Nevertheless, the numerical simulation, *HPHall*, has proven a useful tool for analyzing the physical processes governing Hall thruster operation. Its use is planned for further investigation of this and other problems related to Hall thrusters.

References

- ¹Sankovic, J. M., Hamley, J. A., and T. W. Haag, "Performance Evaluation of the Russian SPT-100 Thruster at NASA LeRC," IEPC-93-094, 23rd International Electric Propulsion Conference, October 1993.
- ²Sankovic, J. M., and T. W. Haag, "Operating Characteristics of the Russian D-55 Thruster with Anode Layer," AIAA-94-3011, 30th AIAA/ASME/SAE/ASEE Joint Propulsion Conference, Indianapolis, Indiana, June 1994.

- ³Lentz, C. A., "Transient One Dimensional Numerical Simulation of Hall Thrusters", Massachusetts Institute of Technology, S.M. Thesis, 1993.

- ⁴Hirakawa, M., and Y. Arakawa, "Particle Simulation of Plasma Phenomena in Hall Thrusters," 24th International Electric Propulsion Conference, Moscow, Russia, 1995.

- ⁵Fife, J. M., and M. Martinez-Sanchez, "Two-Dimensional Hybrid Particle-In-Cell (PIC) Modeling of Hall Thrusters," 24th IEPC, Moscow, Russia, September 1995.

- ⁶Fife, John M., and Manuel Martinez-Sanchez, "Comparison of Results from a Two-Dimensional Numerical SPT Model with Experiment," 32nd AIAA/ASME/SAE/ASEE Joint Propulsion Conference, Lake Buena Vista, FL, 1996.

- ⁷Fife, J. M., Martinez-Sanchez, M., and Szabo, J., "A Numerical Study of Low-Frequency Discharge Oscillations in Hall Thrusters," 33rd AIAA/ASMA/SAE/ASEE Joint Propulsion Conference, Seattle, Washington, July 1997.

- ⁸Fife, J. M., Hybrid-PIC Modeling and Electrostatic Probe Survey of Hall Thrusters, Ph.D. Thesis, Massachusetts Institute of Technology, September 1998.

- ⁹Mitchner and Kruger, Partially Ionized Gasses, John Wiley & Sons, New York, 1973.

- ¹⁰Janes, G. S. and R. S. Lowder, "Anomalous Electron Diffusion and Ion Acceleration in a Low-Density Plasma," Physics of Fluids, 9, P. 1115, 1966.

- ¹¹Bohm, D., Burhop, E.H.S., and Massey, H.S.W., in "Characteristics of Electrical Discharges in Magnetic Fields," A. Guthrie and R. K. Waterling, Eds., McGraw-Hill, New York, 1949.

- ¹²Dugan, John V. and Sovie, Ronald J., "Volume Ion Production Costs in Tenuous Plasmas: A General Atom Theory and Detailed Results for Helium, Argon and Cesium," NASA TN D-4150.

- ¹³Anderson, D. A., Tannehill, J. C., and Pletcher, R. H., Computational Fluid Mechanics and Heat Transfer, Hemisphere Publishing Corporation, New York, 1984.

- ¹⁴Fife, J. M. and M. Martinez-Sanchez, "Characterization of the SPT-70 Plume Using Electrostatic Probes," 34th AIAA/ASMA-/SAE/ASEE Joint Propulsion Conference, Cleveland, Ohio, 1998.

- ¹⁵Komurasaki, K., Hirakawa, M. and Y. Arakawa, "Plasma Acceleration Process in a Hall-Current Thruster", IEPC-91-078, AIDAA/AIAA/DGLR/JSASS 22nd International Electric Propulsion Conference, Viareggio, Italy, Oct. 1991.